International Journal of Bridge Engineering (IJBE), Special Issue 2016, pp. 117-134

DYNAMICS OF AN ARCH BRIDGE UNDER MOVING LOADS

A Mathematical Model

Ioannis G. Raftoyiannis[1] and George T. Michaltsos[2]

[1,2] National Technical University of Athens, Dept. of Civil Engineering, Greece
e-mail: rafto@central.ntua.gr, michalts@central.ntua.gr

ABSTRACT: The present work studies the behavior of an arch bridge under the action of moving loads and proposes a mathematical model for the solution of the problem. The arch bridge under study may have a discontinuous deck or a continuous one, while the columns supporting the deck to the arch are considered as non-extensible. A 2-DOF model is considered for the solution of the bridge while the theoretical formulation is based on a continuum approach, which has been used in the literature to analyze such bridge types.

KEYWORDS: arch bridges; dynamic behavior; moving loads

1 INTRODUCTION

Arches provide a structural system that can efficiently support heavy loads while lending themselves to excellent aesthetics. Historically, arches have been widely used in bridge systems, in modern applications however, they are usually reserved for signature bridges, where aesthetics play an important role in the design. Since arches primarily carry loads through compression, steel as well as concrete are ideal structural materials for these applications.

In the last decades, design practice for various types of steel structures has been changed to limit state design rules in order to obtain more rational designs. Regarding steel arch bridges, there are numerous research papers on the instability design criterion, the creep phenomenon and also their behavior under earthquake actions.

Among the studies related to stability, one should mention the one by Johnston [1] and also those of Bergermeister et al [2], Pircher et al [3], Wang et al [4], Zhu and Sun [5], Bruno et al [6], Mannini et al [7] etc. Among the studies related to the creep phenomenon, there are many [8 to 15] related mainly to the creep of concrete-filled steel arch tubes.

The actual carrying capacity of arches with practical proportioning under realistic earthquake loadings is considerably less than the one related to classical bifurcation buckling [16 to 20]. Finally, there is a lack of publications

related to the support settlement and moving loads.

Regarding the support settlement, Drosopoulos et al [22] studied the behavior of a stone arch bridge subjected to abutment movement, while Liu et al [22] studied the effect of a springing displacement.

As for the moving loads, there are papers related to masonry arch bridges [23] or hanger arch bridges [24-25], while the papers relating to the classical form of an arch bridge (see Fig. 1) employ numerical methods [26] or FEM [27]. Only a few publications study the influence of moving trains, such as the papers of Calcada et al [28], Cher et al [29] or Wallin et al [30].

An arch bridge consists of three elements: the deck, the arch, and the columns that connect deck and arch. There are two main structural systems that are shown in Figs 1a and 1b. The difference lies in the way the deck is supported. In the case of Fig. 1a the deck is discontinuous, while in the case of Fig. 1b the deck is continuous. Each one of the above systems has advantages and disadvantages, while the choice relates for various parameters depending on the environment, where the bridge will be erected.

In the first case of a discontinuous deck, a random load F affects only two neighboring columns (see Fig. 2a), while in the second case of a continuous deck it affects all the columns.

In the following, the columns are considered as non-extensible. A force F acts on the deck at the point x=b and is moving with a constant velocity υ, while the form of the parabolic arch is given by the equation:

$$z(x) = \frac{4 \cdot f_o}{L^2} \cdot x^2 - \frac{4 \cdot f_o}{L} \cdot x \tag{1}$$

The present work studies the behavior of an arch bridge under the action of moving loads and proposes a mathematical model for the problem. The studied arch bridge may have a discontinuous deck or a continuous one, while the columns, connecting deck to arch are considered as non-extensible.

A 2-DOF model is considered for the solution of the bridge while the theoretical formulation is based on a continuum approach, has been used in the literature to analyze such bridges, while the obtained equations are solved using the Duhamel's integrals and the Laplace Transform.

2 THE REACTIONS OF THE COLUMNS

2.1 Discontinuous Deck

Let us consider now the load F moving within points (k-1) to (k+1) of the deck. The so-developed reaction of the column k will be (see Fig. 2a):

$$V_k = F \cdot \left\{ \frac{\upsilon t - \alpha_{k-1}}{\alpha_k - \alpha_{k+1}} \cdot H(\upsilon t - \alpha_{k-1}) \cdot H(\alpha_k - \upsilon t) + \frac{\alpha_{k+1} - \upsilon t}{\alpha_{k+1} - \alpha_k} \cdot H(\upsilon t - \alpha_k) \cdot H(\alpha_{k+1} - \upsilon t) \right\} \tag{2}$$

where H(x-α) is the Heaviside's unit step function.

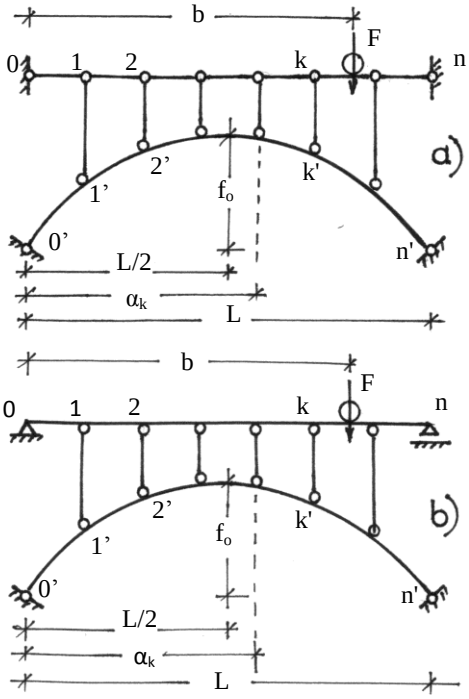

Figure 1. The two static systems

2.2 Continuous Deck

Isolating the deck from the entire bridge and taking into account the columns reactions, we get the model shown in Fig. 2b. The reaction at x=0 is given by the relation:

$$\left.\begin{aligned} V_{bo} &= \frac{F\cdot(L-b)-SV(L)}{L} \\ \text{where:}\quad SV(x) &= \sum_{\rho=1}^{n-1} V_\rho\,(x-\alpha_\rho) \end{aligned}\right\} \qquad (3a)$$

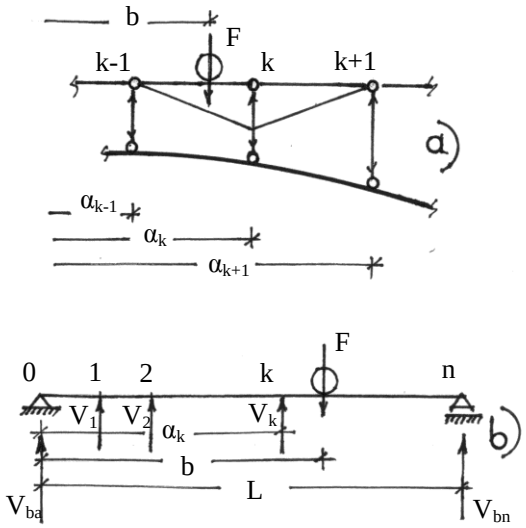

Figure 2. Reaction of columns

and the bending moment M_b is given by the relation:

$$\left.\begin{aligned} &M_b(x) = V_{bo}x + SVa(x) - F\cdot(x-b)\cdot H(x-b) \\ &\text{where:}\quad SVa(x) = \sum_{\rho=1}^{n-1} V_\rho (x-\alpha_\rho)\cdot H(x-\alpha_\rho) \end{aligned}\right\} \quad (3b)$$

Therefore, the equation giving the form of the elastic line will be: $\mathbf{E\,I_b w_b''(x) = -M_b(x)}$, which after a double integration becomes:

$$\left.\begin{aligned} &w_b(x) = A(x) + c_1 x + c_2 \\ &\text{where:}\quad A(x) = -\int\int \frac{M_b(x)}{E\,I_d}\,dx\,dx \end{aligned}\right\} \quad (4)$$

The boundary conditions are:

$$w_b(0) = w_b(L) = 0 \quad (5)$$

which finally give:

$$\left.\begin{aligned} c_1 &= -\frac{A(L)-A(0)}{L} \\ c_2 &= -A(0) \end{aligned}\right\} \quad (6)$$

Isolating now the arch from the entire bridge and taking into account the reactions of the columns, we get the model in Fig. 3.

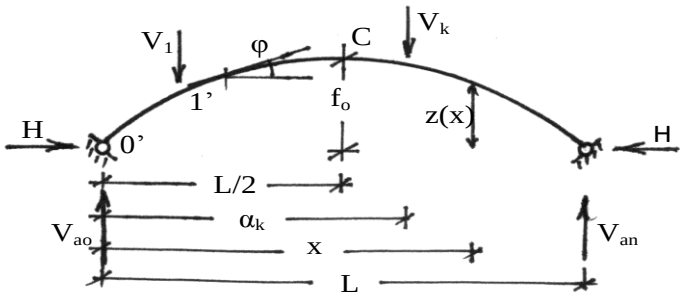

Figure 3. The Arch

The developed reactions at 0' are:

$$\left.\begin{aligned} H &= \frac{1}{4f_o}\sum_{\rho=1}^{n-1} V_\rho \alpha_\rho \left(3-\frac{4\alpha_\rho^2}{L^2}\right) \\ V_{ao} &= \frac{SV(L)}{L} \end{aligned}\right\} \tag{7}$$

The bending moment M_a is:

$$M_a(x) = V_{ao}\cdot x - H\cdot z(x) - SVa(x) \tag{8}$$

Therefore, the equation giving the form of the elastic line will be:

$$E I_a w_a''(x) = -M_a(x) \tag{9}$$

Setting, as usual, $I_a = I_c \cos\varphi$, where I_c the moment of inertia at the top point of the arch (where x=L/2), eq(9) becomes:

$$E I_c w_a''(x) = -M_a(x)\cdot\sqrt{1+z'^2} \tag{10}$$

After a double integration we obtain:

$$\left.\begin{aligned} w_a(x) &= G(x) + d_1\cdot x + d_2 \\ \text{where:}\quad G(x) &= -\iint \frac{M_a(x)\cdot\sqrt{1+z'^2}}{E I_c}\,dx\,dx \end{aligned}\right\} \tag{11}$$

The boundary conditions are:

$$w_a(0) = w_a(L) = 0 \tag{12}$$

which finally give:

$$\left.\begin{aligned} d_1 &= -\frac{G(L)-G(0)}{L} \\ d_2 &= -G(0) \end{aligned}\right\} \tag{13}$$

The deck beam and the arch are connected through the pinned columns. Therefore, the following conditions are valid:

$$\left.\begin{aligned} & w_b(\alpha_1) = w_a(\alpha_1) \\ & \cdots\cdots\cdots\cdots\cdots\cdots \\ & w_b(\alpha_k) = w_a(\alpha_k) \\ & \cdots\cdots\cdots\cdots\cdots\cdots \\ & w_b(\alpha_{n-1}) = w_a(\alpha_{n-1}) \end{aligned}\right\} \tag{14}$$

From the above system of eqs (14), the stresses V_1,..., V_{n-1} of the columns can be determined.

3 THE ARCH

Let us consider the arch beam of figure 4, that is based on points 1 and 2 and its form is given by the following equation:

$$z = z(x) \tag{15a}$$

From the initial and the deformed state of an infinitesimal part ds of the arch we find:

$$\left.\begin{aligned} dx + du &= (1+\varepsilon)\cdot ds\cdot\cos(\varphi+\psi) \cong dx + \varepsilon\cdot dx - \psi\cdot dz \\ dz + dw &= (1+\varepsilon)\cdot ds\cdot\sin(\varphi+\psi) \cong dz + \varepsilon\cdot dz + \psi\cdot dx \end{aligned}\right\}$$

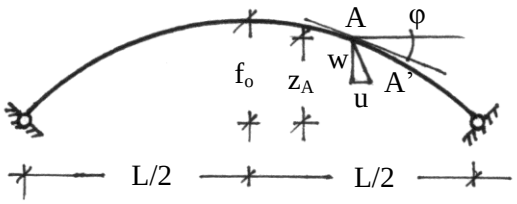

Figure 4. The arch

or finally:

$$\left.\begin{aligned} du &= \varepsilon\cdot dx - \psi\cdot dz \\ dw &= \psi\cdot dx + \varepsilon\cdot dz \end{aligned}\right\} \tag{15b}$$

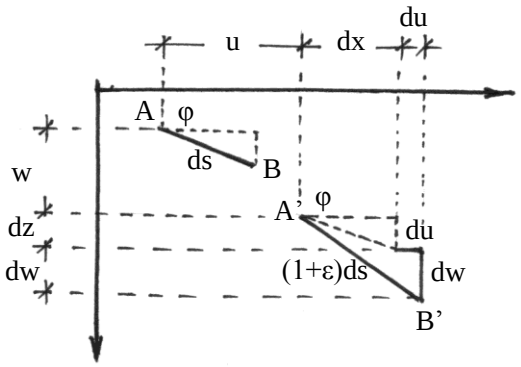

Figure 5. Deformation of an infinitesimal part ds

where, infinitesimals of higher order $(\varepsilon \cdot dz \cdot \psi,\ \ \varepsilon \cdot dz \cdot dx)$ are neglected. For a non-extensible beam (ε=0) we have:

$$\left.\begin{aligned} \frac{d\psi}{ds} &= \frac{d^2 w}{dx^2} \cdot \frac{dx}{ds} \\ \frac{du}{dx} &= \varepsilon \cdot \left[1 + \left(\frac{dz}{dx}\right)^2\right] - \frac{dw}{dx} \cdot \frac{dz}{dx} \end{aligned}\right\} \qquad (15c)$$

From the second of the above eqs (15c) we obtain:

$$\int_0^L du = u(L) - u(0) = \int_0^L \varepsilon \cdot (1 + z'^2) dx - \int_0^L z' \cdot w' dx = 0$$

which after integration gives (because $w(0) = w(L) = u(0) = 0$):

$$\int_0^L \varepsilon \cdot (1 + z'^2) dx + \int_0^L z'' \cdot w dx = 0 \qquad (15d)$$

On the other hand, we know that:

$$\left.\varepsilon = \frac{N}{E \cdot A(x)},\quad 1 + z'^2 = \frac{1}{\cos^2 \varphi},\quad N = \frac{H}{\cos \varphi}\right\} \qquad (15e)$$

therefore, equation (15d) becomes:

$$\int_0^L \frac{N}{E \cdot A(x) \cdot \cos^2 \varphi} dx = \int_0^L \frac{H}{E \cdot A(x) \cdot \cos^3 \varphi} dx = -\int_0^L z'' \cdot w dx \qquad (15f)$$

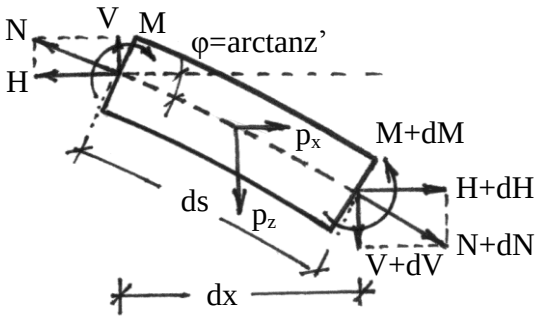

Figure 6. Equilibrium of an infinitesimal part ds

From Fig. 6, we get $dH = -p_x dx$ and because it is usually $p_x = 0$, we obtain:

$$H = \text{constant} \tag{16a}$$

and thus:

$$\left.\begin{aligned} H &= -\frac{1}{K}\cdot\int_0^L z''\cdot w dx \\ \text{where: } K &= \int_0^L \frac{dx}{EA(x)\cos^3\varphi} \end{aligned}\right\} \tag{16b}$$

From the equilibrium of Fig. 6, we conclude to the following equations:

$$\left. z''H = -p_z\,,\quad \frac{dV}{dx} = -p_z\,,\quad \frac{d^2M}{dx^2} = H\cdot(z-w)'' + p_z \right\} \tag{16c}$$

From the first of (15c) we get: $\frac{d\psi}{ds} = \frac{d^2w}{dx^2}\cdot\frac{dx}{ds} = -\frac{M}{EI_a}$

or $\frac{d^2w}{dx^2} = -\frac{M}{EI_a\cos\varphi}$ or because of eq(16c):

$\frac{d^2}{dx^2}\left(EI_a\cos\varphi\frac{d^2w}{dx^2}\right) = H\cdot(z-w)'' + p_z$ and taking into account equation eq (16d) and the inertia forces, we get:

$$\frac{d^2}{dx^2}\left(EI_a\cos\varphi\frac{d^2w}{dx^2}\right) + H\cdot w'' + m\ddot{w} = p_z - \frac{z''}{K}\cdot\int_0^L z''\cdot w dx \tag{16d}$$

From eq (1), we find $z'' = 8f_o / L^2$ while we set, as usual, $I_a\cos\varphi = I_c$ where I_c

is the moment of inertia at the top point of the arch. Therefore, eq (16d) becomes:

$$E I_c w'''' - \frac{mgL^2}{8f_o} w'' + m\ddot{w} = p_z - \frac{64 f_o^2}{KL^4} \int_0^L w dx \tag{16e}$$

3.1 The free vibrating arch

With $p_z = 0$, the equation of the free motion is:

$$E I_c w'''' - \frac{mgL^2}{8f_o} w'' + m\ddot{w} = -\frac{64 f_o^2}{KL^4} \int_0^L w dx \tag{17a}$$

We are searching for a solution of the form:

$$w(x,t) = W(x) \cdot e^{i\omega t} \tag{17b}$$

Therefore, eq (17a) becomes:

$$\left.\begin{aligned} & W'''' - A \cdot W'' - k^4 W = -B \int_0^L W\, dx \\ & \text{where:} \quad A = \frac{mgL^2}{8 f_o E I_c}, \quad B = \frac{64 f_o^2}{K L^4 E I_c}, \quad k^4 = \frac{m\omega^2}{E I_c} \end{aligned}\right\} \tag{17c}$$

Given that the integral of the right site member is independent of x, the general solution of eq (17c) will be:

$$\left.\begin{aligned} & W(x) = c_1 \sin\lambda_1 x + c_2 \cos\lambda_1 x + c_3 \mathrm{Sinh}\lambda_2 x + c_4 \mathrm{Cosh}\lambda_2 x + \frac{B}{k^4} \int_0^L W dx \\ & \text{with:} \quad \lambda_1 = \sqrt{-\frac{A}{2} + \sqrt{\frac{A^2}{4} + k^4}}, \quad \lambda_2 = \sqrt{\frac{A}{2} + \sqrt{\frac{A^2}{4} + k^4}} \end{aligned}\right\} \tag{17d}$$

Integrating eq (17d) we find:

$$\int_0^L W dx = \frac{k^4}{k^4 - BL} \cdot \left[-\frac{c_1}{\lambda_1}(\cos\lambda_1 L - 1) + \frac{c_2}{\lambda_1} \sin\lambda_1 L + \frac{c_3}{\lambda_2}(\mathrm{Cosh}\lambda_2 L - 1) + \frac{c_4}{\lambda_2} \mathrm{Sinh}\lambda_2 L \right]$$

Therefore, the final solution of eq (17c) becomes:

$$W(x) = c_1\left[\sin\lambda_1 x - \frac{B}{\lambda_1(k^4 - BL)}(\cos\lambda_1 L - 1)\right] + c_2\left[\cos\lambda_1 x + \frac{B}{\lambda_1(k^4 - BL)}\sin\lambda_1 L\right]$$
$$+ c_3\left[\mathrm{Sinh}\lambda_2 x + \frac{B}{\lambda_2(k^4 - BL)}(\mathrm{Cosh}\,\lambda_2 L - 1)\right] + c_4\left[\mathrm{Cosh}\lambda_2 x + \frac{B}{\lambda_2(k^4 - BL)}\mathrm{Sinh}\lambda_2 L\right] \Bigg\} \tag{17e}$$

With boundary conditions $W(0) = W(L) = W''(0) = W''(L) = 0$, we obtain the following equation for eigenfrequencies:

$$\begin{vmatrix} -\frac{B}{\lambda_1(k^4 - BL)}(\cos\lambda_1 L - 1) & \left(1 + \frac{B}{\lambda_1(k^4 - BL)}\sin\lambda_1 L\right) & \frac{B}{\lambda_2(k^4 - BL)}(\mathrm{Cosh}\lambda_2 L - 1) & \left(1 + \frac{B}{\lambda_2(k^4 - BL)}\mathrm{Sinh}\lambda_2 L\right) \\ \sin\lambda_1 L & \cos\lambda_1 L - 1 & \mathrm{Sinh}\lambda_2 L & \mathrm{Cosh}\lambda_2 L - 1 \\ 0 & -\lambda_1^2 & 0 & \lambda_2^2 \\ -\lambda_1^2\sin\lambda_1 L & -\lambda_1^2\cos\lambda_1 L & \lambda_2^2\mathrm{Sinh}\lambda_2 L & \lambda_2^2\mathrm{Cosh}\lambda_2 L \end{vmatrix} = 0 \tag{18a}$$

Finally, the shape functions are given by (17e) with:

$$\left.\begin{aligned} c_2 &= -c_1 \cdot \frac{\sin\lambda_1 L}{\cos\lambda_1 L - 1} \\ c_3 &= c_1 \cdot \left(\frac{\lambda_1}{\lambda_2}\right)^2 \cdot \frac{\sin\lambda_1 L \cdot (\mathrm{Cosh}\lambda_2 L - 1)}{\mathrm{Sinh}\lambda_2 L \cdot (\cos\lambda_1 L - 1)} \\ c_4 &= -c_1 \cdot \left(\frac{\lambda_1}{\lambda_2}\right)^2 \cdot \frac{\sin\lambda_1 L}{\cos\lambda_1 L - 1} \end{aligned}\right\} \tag{18b}$$

3.2 The forced vibrating arch

Equation (16e) can be written as follows:

$$E I_c w'''' - \frac{mgL^2}{8f_o} w'' + m\ddot{w} = \sum_{\rho=1}^{n-1} V_\rho(b)\,\delta(x - \alpha_\rho) - \frac{64 f_o^2}{KL^4}\int_0^L w\,dx \tag{19a}$$

where $\delta(x\text{-}a)$ the Dirac delta function.
We are searching for a solution of the form:

$$w(x,t) = \sum_n W_n(x)\cdot T_n(t) \tag{19b}$$

where $W_n(x)$ are the shape functions of §3.1 and $T_n(t)$ the time functions under

determination. Introducing (19b) into (19a) we obtain:

$$E I_c \sum_n W_n'''' T_n - \frac{mgL^2}{8f_o} \sum_n W_n'' T_n + m \sum_n W_n \ddot{T}_n = \sum_{\rho=1}^{n-1} V_\rho(b)\,\delta(x-\alpha_\rho) - \frac{64 f_o^2}{KL^4} \int_0^L \sum_n W_n T_n dx$$

Remembering that W_n satisfies the equation of free motion (17c), the above becomes:

$$m \sum_n W_n \ddot{T}_n + m \sum_n \omega_n^2 W_n T_n = \sum_{\rho=1}^{n-1} V_\rho(b)\,\delta(x-\alpha_\rho).$$

Multiplying the above by W_k, integrating the outcome from 0 to L and taking into account the orthogonality condition, we obtain:

$$\ddot{T}_k + \omega_k^2 T_k = \frac{1}{m\int_0^L W_k^2 dx} \cdot \int_0^L \sum_{\rho=1}^{n-1} V_\rho(b)\, W_k(x)\delta(x-\alpha_\rho)\,dx = \frac{1}{m\int_0^L W_k^2 dx} \cdot \sum_{\rho=1}^{n-1} V_\rho(b) W_k(\alpha_\rho) \qquad (19c)$$

Since $b = \upsilon \cdot t$ i.e. $V_\rho(b)$ is a function of t, the solution of the above (19c) is given by the Duhamel's integral:

$$T_k(t) = \frac{1}{\omega_k m\int_0^L W_k^2 dx} \cdot \int_0^t \sum_{\rho=1}^{n-1} V_\rho(\upsilon\cdot\tau)\cdot W_k(\alpha_\rho)\cdot \sin[\omega_k(t-\tau)]\,d\tau \qquad (19d)$$

4 NUMERICAL EXAMPLES AND DISCUSSION

Let us consider an arch bridge with length L=200m (see Fig. 7).
The bridge consists:

a) From the deck that has static form either of a continuous beam (fig. 7b) or it is composed from simply supported beams (Fig. 7a).
b) From the pinned-pinned arch and
c) From four pinned-pinned columns that connect the deck to the arch.

The bridge is made from structural steel (isotropic and homogeneous material), with modulus of elasticity $E=2.1*10^8$ kN/m^2.

The deck (a continuous beam or a discontinuous one) has five equal spans of 40m length, that means that the needed distances α_i will be: $\alpha_o = 0$, $\alpha_1 = 40$, $\alpha_2 = 80$, $\alpha_3 = 120$, $\alpha_4 = 160\,m$, and $\alpha_5 = 200\,m$. Its mass is $m_d = 400\,kg/m$ and its moment of inertia $I_d = 0.02\,m^4$.

The arch is s pinned-pinned one with the following characteristics: L=200 m, f_o=70 m, I_c=0.8 m^4, m_a=800 kg/m and $A(x) \cong 1.22\,m^2$.

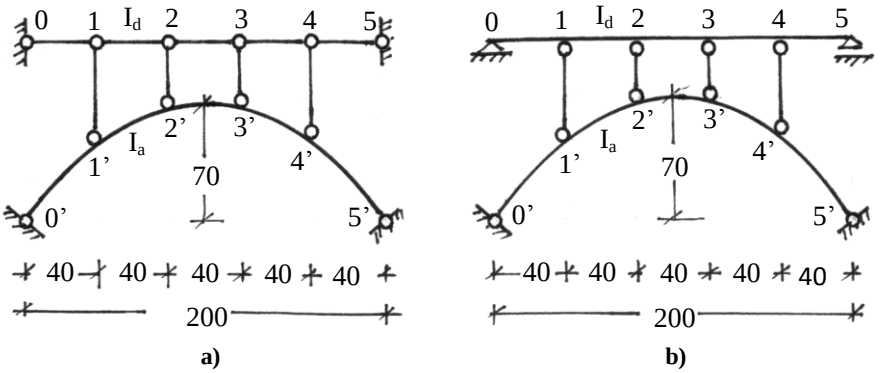

Figure 7. The studied systems

We will study the behavior of the two static systems, as they are described above, for the case of a load P=500 kN, moving with speeds $\upsilon = 10, 20, \text{and } 30\,\text{m/sec}$ (i.e. 36, 72, and 108 km/h).

Applying equation (18a) we determine the following first four eigenfrequencies of the arch: $\omega_1 = 4.600\,\text{sec}^{-1}$, $\omega_2 = 9.525\,\text{sec}^{-1}$, $\omega_3 = 18.169\,\text{sec}^{-1}$, and $\omega_4 = 40.738\,\text{sec}^{-1}$.

4.1 The system of Figure 7a

Applying the equations (2), we obtain the following plots showing the acting forces on each one of the four columns of the bridge.

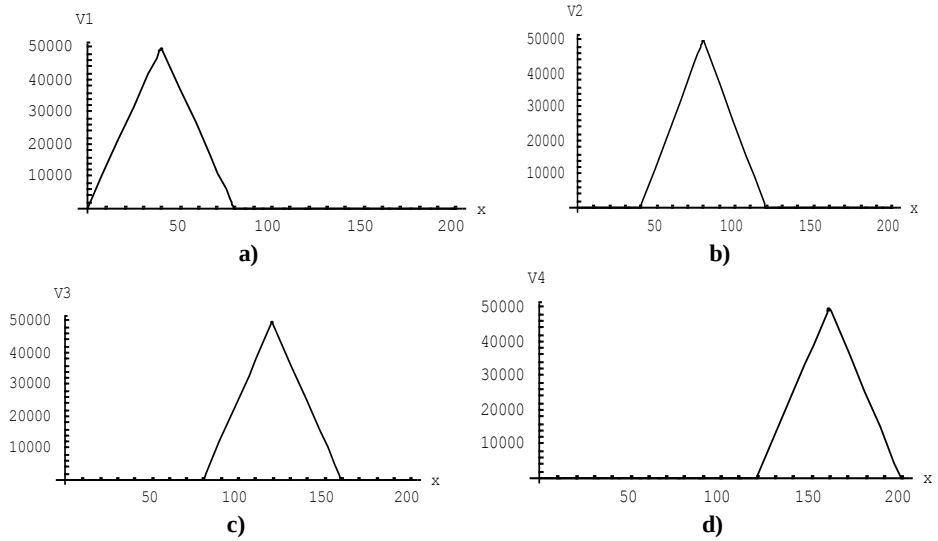

Figure 8. Stresses of the columns 1-1 (a), 2-2 (b), 3-3 (c) and 4-4 (d)

Easily, we ascertain that the moving load affects each time only two neighbor columns.

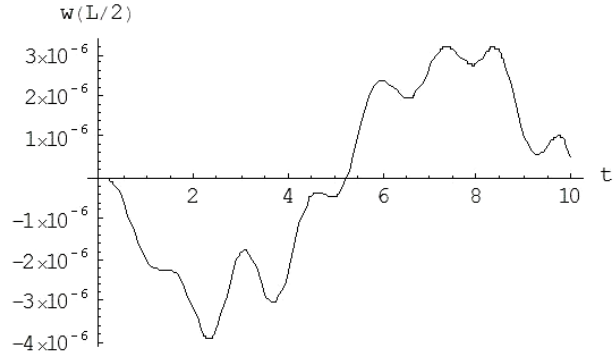

Figure 9. Displacements of the middle of the arch for speed υ=10m/sec

From the equations (17e), (18b), (19b) and (19d), we get the plots of figures 9 and 10, where they are shown the displacement of the middle of the arch and the ones of the points 1', 2', 3', and 4', where the columns are joined to the arch.

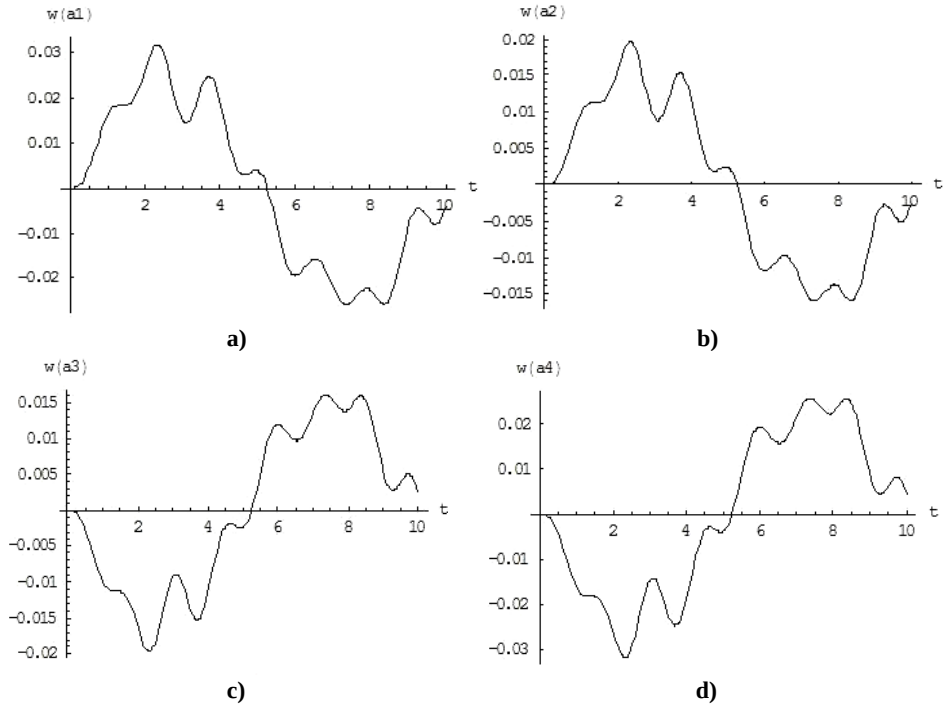

Figure 10. Displacements of the points 1' (a), 2' (b), 3' (c) and 4' (d) of the arch for speed υ=10m/sec

As it is clear the displacement of the middle of the arch is practically zero. This is an expected result. Another result is that the maximum displacement of the arch occurs when the load is located on the first column.

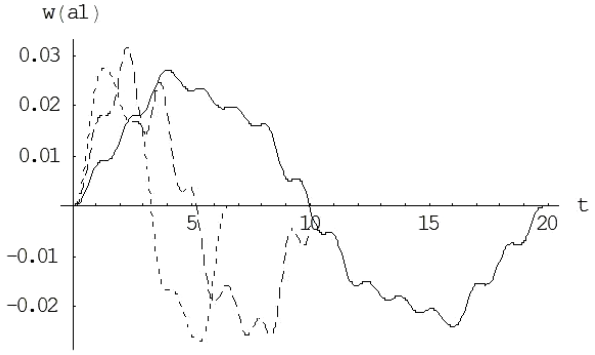

Figure 11. Displacements of the point 1' of the arch for speeds υ=10 (___), 20 (_ _) and 30 m/sec (- - -)

For this reason the plots of Fig. 11 show the displacements of the point 1' of the arch, where the first column is joined to it, for different speeds of the moving load.

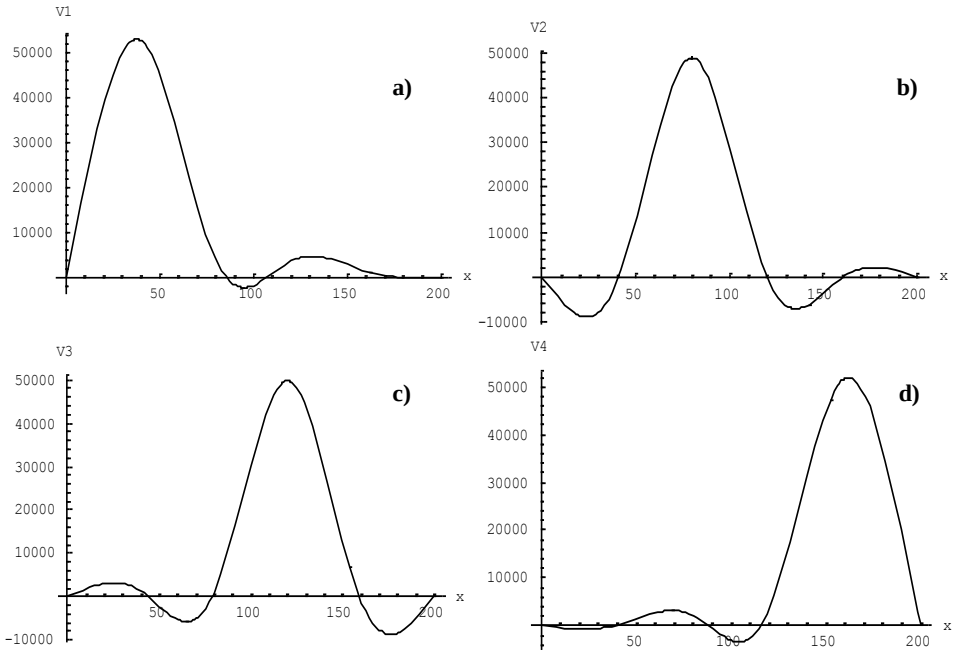

Figure 12. Stresses of the columns 1-1 (a), 2-2 (b), 3-3 (c) and 4-4 (d)

4.2 The system of Figure 7b

Applying the previously exposed in §2.2 procedure, we obtain the following plots showing the acting forces on each one of the four columns of the bridge.

Contrarily to the previous studied system of a discontinuous deck we see that the moving load affects all the columns and not only the two neighboring ones.

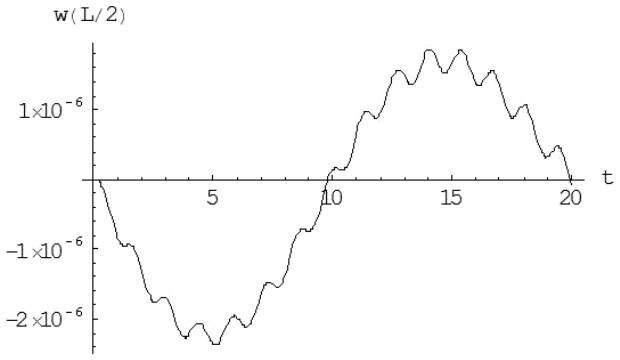

Figure 13. Displacements of the middle of the arch for speed υ=10m/sec

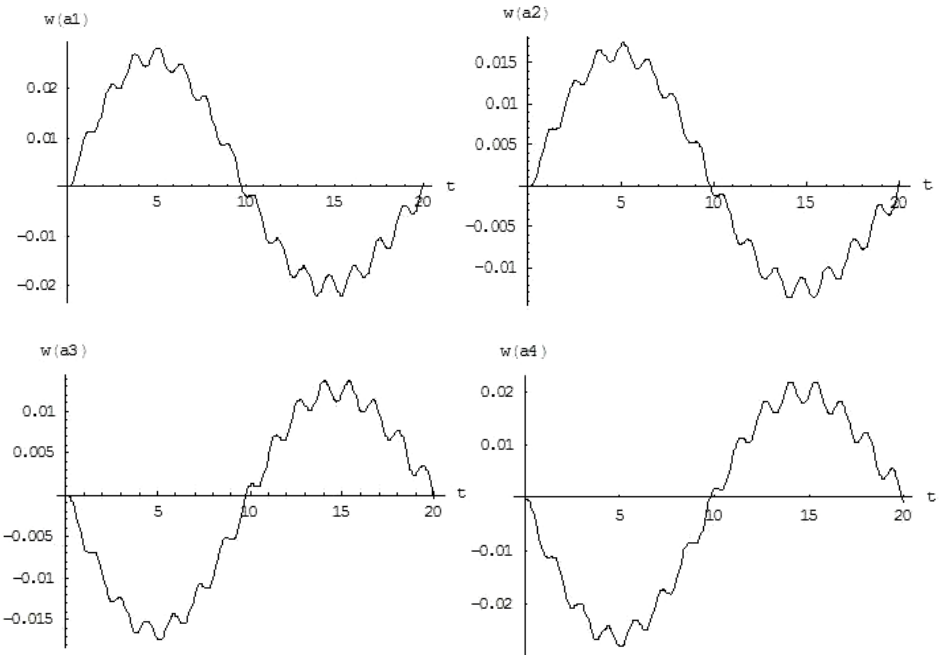

Figure 14. Displacements of the points 1' (a), 2' (b), 3' (c) and 4' (d) of the arch for speed υ=10m/sec

From the equations (17e), (18b), (19b) and (19d), we get the plots of figures 13 and 14, where they are shown the displacement of the middle of the arch and the ones of the points 1', 2', 3', and 4', where the columns are joined to the arch.

As it is clear the displacement of the middle of the arch for the case of a continuous deck is also substantially null. This is an expected result.

For the case of the continuous deck, we get the same result that the maximum displacement of the arch is happened when the load is located on the first column.

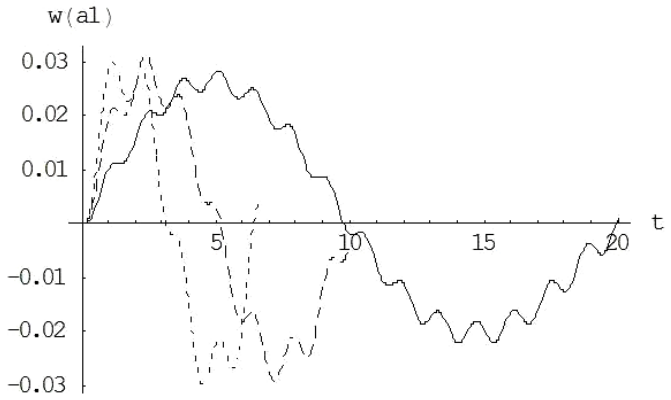

Figure 15. Displacements of the point 1' of the arch for speeds υ=10 (___), 20 (_ _) and 30 m/sec (- - -)

For this reason we draw the plots of figure 15 where they are shown the displacements of the point 1' of the arch, where the first column is joined to it, for different speeds of the moving load.

5 CONCLUSIONS

A mathematical model is proposed herein for the two static systems of an arch bridge of over passing under the action of moving loads.

From the results of the models considered, one can draw the following conclusions.

1. The static model affects the stress of the columns. Using the model of discontinuous deck, the moving load affects, each time, only two neighboring columns. Contrarily, using the model of continuous deck, we see that the moving load affects all the columns and not only the two neighboring ones.
2. The middle of the bridge for both static systems has negligible displacements (practically zero).
3. The maximum displacements of the arch occur when the load is moving at

intervals $L/5 \le x \le 2L/5$ or $3L/5 \le x \le 4L/5$ for both static systems.

4. The stress of the columns is greater in the continuous system. This difference amounts in about 5%.
5. The displacements appeared in the discontinuous system are greater than the ones appeared in the continuous one. The difference depends on the speed of the moving load and decreases as the speed increases.

REFERENCES

1. Johnston B.G. "Guide to stability design criteria for metal structures", Structural Stability Research Council, 3rd edition, John Wiley & Sons, N.Y., 1976
2. Bergmeister, K., Capsoni, A., Corradi, L., Menardo, A. "Lateral elastic stability of slender arches for bridges including deck slenderness", Structural Engineering International: Journal of the International Association for Bridge and Structural Engineering (IABSE), 19 (2), pp. 149-154, 2009
3. Pircher, M., Stacha, M., Wagner, J. "Stability of network arch bridges under traffic loading" Proceedings of the Institution of Civil Engineers: Bridge Engineering 166 (3), pp. 186-192, 2013
4. Wang, Y., Liu, C., Liang, Y., Zhang, S. "Nonlinear stability analysis and completed bridge test on slanting type CFST arch bridges", Source of the Document Jianzhu Jiegou Xuebao/Journal of Building Structures 36, pp. 107-113, 2015
5. Zhu, X.-L., Sun, D.-B. "Nonlinear in-plane stability and catastrophe analysis of shallow arches", Zhendong yu Chongji/Journal of Vibration and Shock 35 (6), pp. 47-51 and 74, 2016
6. Bruno, D., Lonetti, P., Pascuzzo, A. "Document An optimization model for the design of network arch bridges", Computers and Structures 170, pp. 13-25, 2016
7. Mannini, C., Belloli, M., Marra, A.M., (...), Robustelli, F., Bartoli, G. "Aeroelastic stability of two long-span arch structures: A collaborative experience in two wind tunnel facilities", Engineering Structures 119, pp. 252-263, 2016
8. Zhang, Z.-C. "Creep analysis of long span concrete-filled steel tubular arch bridges", Gongcheng Lixue/Engineering Mechanics 24 (5), pp. 151-160, 2007
9. Shao, X., Peng, J., Li, L., Yan, B., Hu, J. "Time-dependent behavior of concrete-filled steel tubular arch bridge", Journal of Bridge Engineering 15 (1), pp. 98-107, 2010
10. Loghman, A., Ghorbanpour Arani, A., Shajari, A.R., Amir, S. "Time-dependent thermoelastic creep analysis of rotating disk made of Al-SiC composite", Archive of Applied Mechanics 81 (12), pp. 1853-1864, 2011
11. Lai, X.-Y., Li, S.-Y., Chen, B.-C., "The influence of addictives on the creep of concrete-filled steel tube", Harbin Gongye Daxue Xuebao/Journal of Harbin Institute of Technology 44 (SUPPL.1), pp. 248-251, 2012
12. Granata, M.F., Arici, M. "Serviceability of segmental concrete arch-frame bridges built by cantilevering", Bridge Structures 9 (1), pp. 21-36, 2013
13. Ma, Y.S., Wang, Y.F. "Creep effects on the reliability of a concrete-filled steel tube arch bridge", Journal of Bridge Engineering 18 (10), pp. 1095-1104, 2013
14. Zhou, Y. "Concrete creep and thermal effects on the dynamic behavior of a concrete-filled steel tube arch bridge", Journal of Vibroengineering 16 (4), pp. 1735-1744, 2014
15. Bradford, M.A., Pi, Y.-L. "Geometric Nonlinearity and Long-Term Behavior of Crown-Pinned CFST Arches", Journal of Structural Engineering (United States) 141 (8), 04014190, 2015
16. Li, J.-B., Ge, S.-J., Chen, H. "Document Seismic behavior analysis of a 5-span continuous half-through CFST arch bridge", World Information on Earthquake Engineering 21(3) pp110-115, 2005

17. Álvarez, J.J., Aparicio, A.C., Jara, J.M., Jara, M. "Seismic assessment of a long-span arch bridge considering the variation in axial forces induced by earthquakes", Engineering Structures 34, pp. 69-80, 2012
18. Huang, F.-Y., Chen, B.-C., Li, J.-Z., Cheng, H.-D. "Shaking tables testing of concrete filled steel tubular single arch rib model under the excitation of rare earthquakes", Gongcheng Lixue/Engineering Mechanics 32 (7), pp. 64-73, 2015
19. Sevim, B., Atamturktur, S., Altunişik, A.C., Bayraktar, A. "Ambient vibration testing and seismic behavior of historical arch bridges under near and far fault ground motions", Bulletin of Earthquake Engineering , 14(1), 241-259, 2016
20. Lei, S., Gao, Y., Pan, D. "An optimization solution of Rayleigh damping coefficients on arch bridges with closely-spaced natural frequencies subjected to seismic excitations", Harbin Gongye Daxue Xuebao/Journal of Harbin Institute of Technology 47 (12), pp. 123-128, 2015
21. Drosopoulos, G.A., Stavroulakis, G.E., Massalas, C.V. "Influence of the geometry and the abutments movement on the collapse of stone arch bridges", Construction and Building Materials 22 (3), pp. 200-210, 2008
22. Liu, B., Yang, C., Zhou, K. "Document Effect of springing displacement on mechanical performance of the buried corrugated steel arch bridge", Wuhan Ligong Daxue Xuebao (Jiaotong Kexue Yu Gongcheng Ban)/Journal of Wuhan University of Technology (Transportation Science and Engineering) 36 (3), pp. 441-444, 2012
23. Liu, S.-M., Wang, Z.-X., Zhu, C. "Method of temporarily carrying heavy vehicle on masonry arch bridge without strengthening", Beijing Gongye Daxue Xuebao/Journal of Beijing University of Technology 41 (10), pp. 1559-1565, 2015
24. Yau, J.-D. "Vibration of parabolic tied-arch beams due to moving loads", Document International Journal of Structural Stability and Dynamics, 6 (2), pp. 193-214, 2006
25. Yang, J.-X., Chen, W.-Z., Gu, R. "Analysis of dynamic characteristics of short hangers of arch bridge", Bridge Construction 44 (3), pp. 13-18, 2014
26. Nikkhoo, A., Kananipour, H., "Document Numerical solution for dynamic analysis of semicircular curved beams acted upon by moving loads", Proceedings of the Institution of Mechanical Engineers, Part C: Journal of Mechanical Engineering Science 228 (13), pp. 2314-2322. 2014
27. Türker, T., Bayraktar, A. "Structural safety assessment of bowstring type RC arch bridges using ambient vibration testing and finite element model calibration", Measurement: Journal of the International Measurement Confederation pp 33-45, 2014
28. Calçada, R., Cunha, A., Delgado, R., "Dynamic analysis of metallic arch railway bridge", Journal of Bridge Engineering 7 (4), pp. 214-222, 2002
29. Chen, S., Tang, Y., Huang, W.-J., "Visual vibration simulation of framed arch bridge under multi-vehicle condition", Gongcheng Lixue/Engineering Mechanics 22 (1), pp. 218-222, 2005
30. Wallin, J., Leander, J., Karoumi, R. "Strengthening of a steel railway bridge and its impact on the dynamic response to passing trains", Engineering Structures 33 (2), pp. 635-646, 2011